ChemComm

Accepted Manuscript

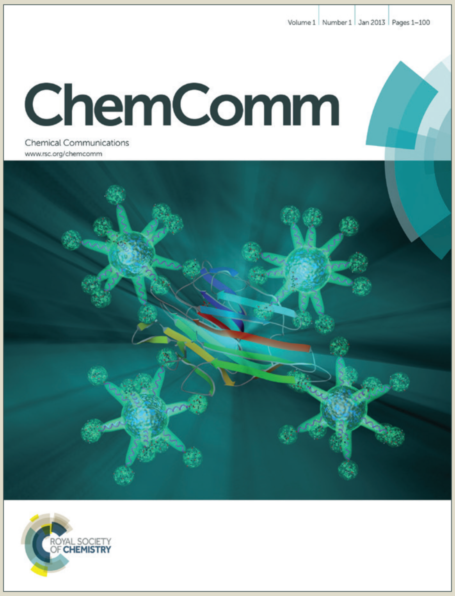

ROYAL SOCIETY OF CHEMISTRY

www.rsc.org/chemcomm

Cite this: DOI: 10.1039/c0xx00000x

www.rsc.org/xxxxxx

ARTICLE TYPE

Mechanically reinforced phosphoric acid doped quaternized poly (ether ether ketone) membranes via cross-linking with functionalized graphene oxide

Na Zhang, Baolong Wang, Yurong Zhang, Fanzhe Bu, Ying Cui, Xuefeng Li, Chengji Zhao* and Hui Na*

Received (in XXX, XXX) Xth XXXXXXXXX 20XX, Accepted Xth XXXXXXXXX 20XX
DOI: 10.1039/b000000x

Functionalized graphene oxide (FGO) reinforced quaternized poly(ether ether ketone) membranes were prepared for high temperature proton exchange membrane. The introduction of FGO significantly improved the mechanical strength and oxidative stability of these membranes at a high doping level. These reinforced membranes showed high tensile strength up to 40 MPa and high proton conductivity up to 58 mS cm^{-1} at 200 °C.

Fuel cells (FCs), which can convert chemical energy into electric energy directly without releasing toxic substances, are attracting more and more attention around the world because of environmental pollution and energy shortage [1]. Proton exchange membrane fuel cell (PEMFC), which is mainly composed of cathode, anode and proton exchange membrane (PEM), is one kind of fuel cells. PEM is the core of the PEMFC. At present, commercial PEMs are perfluorosulfonic membranes represented by Nafion series. Nafion possesses excellent chemical, dimensional stability and high proton conductivities when hydrated at low temperatures (<80 °C). However, when the temperature is higher than 80 °C, tensile strength and dimensional stability of Nafion become very bad, which leads to its uselessness [2]. There are many advantages for PEMFC operating at high temperature (Here, the high temperature usually is 100-200 °C.), including enhanced electrochemical kinetics, simplified water and heat management, utilization of non-platinum catalyst and higher CO-rich reformed hydrogen [3]. The PEM used for high temperature proton exchange membrane fuel cell (HTPEMFC) has been a hot research point in the field of FCs.

At present, the most widely studied HTPEM is phosphoric acid (PA) doped polybenzimidazole (PBI) membrane [4]. PBI possesses high thermal stability and tensile strength because of intermolecular hydrogen bonds. Alternative material of HTPEM is aromatic poly(ether ketone/sulfone) bearing polar functional groups or N-heterocycle on main-chain or side-chain. The aromatic poly(ether ketone/sulfone) also has excellent thermal stability and is relatively cheap. And the PA doping level can be controlled by the amount of polar functional groups. So far, there have been many researches about aromatic poly(ether ketone/sulfone) used as HTPEMs [5]. For example, Kallitsis' group prepared a series of aromatic polyether containing pyridine units on the main-chain for high temperature fuel cell application [6].

In recent years, graphene oxide (GO) and functionalized graphene oxide (FGO) as inorganic fillers in polymer composites have attracted more and more attention. Because the surface of GO is covered with hydroxyl, epoxy and carboxyl groups, which could form hydrogen-bond channels for proton conduction. The proton conductivity of GO is up to 10^{-4} S cm^{-1} [7]. Furthermore, Tateishi *et al*. prepared a graphene oxide fuel cell with GO paper as the electrolyte [8]. Ravikumar *et al*. prepared sulfonated graphene oxide paper as a new polymer electrolyte for fuel cell [9]. The GO or FGO as inorganic fillers showed excellent performance in field of low and high temperature PEM. Lin *et al*. prepared GO-laminated Nafion 115 membrane for direct methanol fuel cell, the GO-laminated Nafion membrane showed lower methanol permeability and better cell performance compared with Nafion 115 membrane [10]. He *et al*. studied the various size GO and sulfonated polyimide (SPI) composite membranes. They found that the incorporation of GO improved mechanical properties and proton conductivity while reducing methanol permeability [11]. Xu *et al*. prepared PBI/GO and PBI/sulfonated GO composite membranes used as PA doped HTPEM. The SGO/PBI/PA exhibited a proton conductivity of 0.052 S cm^{-1}, which was higher than those of GO/PBI/PA (0.027 S cm^{-1}) and PBI/PA (0.023 S cm^{-1}) membranes [12].

Here, quaternized poly(ether ether ketone) (QPEEK) was prepared to be doped with phosphoric acid, using as a HTPEM. However, the PA doped QPEEK membrane was excessively swollen at high doping levels and tensile strength was too low to keep membrane integrity. Therefore, we proposed to introduce GO into QPEEK membrane to improve tensile strength, because GO could form hydrogen-bond network structure in membrane, which not only could improve the tensile strength but also provide the sites for proton conduction. However, it is well known that GO has a much poor dispersion in organic solvent, making it difficult to achieve a well-dispersed composite membrane. In order to improve the compatibility of GO and QPEEK, *p*-aminobenzene sulfonic acid was introduced into GO to obtain functionalized GO (FGO) by the reaction between epoxy group of GO and the amine group of *p*-aminobenzene sulfonic acid. FGO has a good dispersion in dimehyl sulphoxide and could form ionic bond with QPEEK. Both the QPEEK-*x*%GO and QPEEK-*x*%FGO membranes had been prepared, where the *x*% stood for the weight percentage of GO or FGO.

QPEEK was synthesized by quaterization of bromomethylated poly(ether ether ketone) (Br-PEEK) with 1-methylimidazole. The nuclear magnetic resonance spectra of Br-PEEK and QPEEK are shown in Figure S1. In the spectrum of Br-PEEK, the peak at δ_H=4.5 ppm belongs to the benzyl group. The peak at δ_H=2.2 ppm relates to the methyl groups. The chemical shifts of hydrogen atoms on the benzene rings appear at 7.8-6.9 ppm. According to the integral peak area, the degree of bromo-substitution is 43 %. After the quaterization reaction, the chemical shift of benzyl group transfers to 5.4 ppm, while the peak at δ_H=4.5 ppm disappears completely. The new peaks at δ_H=9.1-9.0 ppm, δ_H=7.9 ppm, δ_H=7.6 ppm and δ_H=3.7 ppm corresponding to the methylimidazole appear in the spectrum of QPEEK. The results confirmed that the conversion of benzyl bromide groups to imidazolium groups was almost complete.

X-ray photoelectron spectroscopy (XPS) and X-ray diffraction (XRD) were used to determine the chemical structure of GO and FGO, further verifying whether the reaction took place or not. Figure 1 (a, b) shows the C1s narrow scan spectra of GO and FGO. The carbon signal is divided into four signals, including C in graphite (284.6 eV), C-OH (285.2 eV), C in epoxy (286.8 eV) and C=O (288.5 eV), which are identical with the results of previous work [13]. Comparing with XPS spectrum of GO, the C1s narrow scan spectra of FGO do not exhibit new peak. But, the shapes of all peaks have changed. In Figure 1b, the peak intensity of C in epoxy decreases dramatically after the reaction of GO with *p*-aminobenzene sulfonic acid. The C in epoxy group (C-O-C) is converted to C-OH group and C-N group as shown in Scheme 1. Therefore, the peak intensity of C in C-OH increases. The peak intensity of C in epoxy decreases sharply.

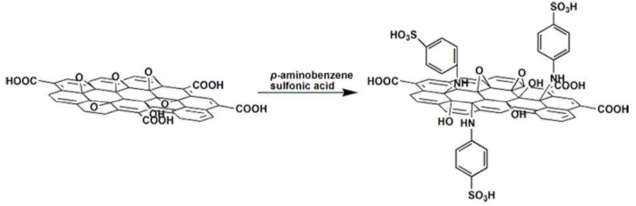

Scheme 1. The preparation of FGO.

The XRD patterns of GO and FGO are shown in Figure 1c. The diffraction peak at 2θ=12.8° corresponds to the plane (001) reflection of GO, which shows the interlayer spacing is 0.69 nm. The peak at 2θ=26.8° belongs to graphite whose interlayer spacing is 0.33 nm. The results are close to those of previous work [14]. GO has a larger interlayer spacing than graphite because of the existence of oxygen-containing functional groups. When the *p*-aminobenzene sulfonic acid was inserted to the interlays, the interlay spacing would become larger. The interlay spacing of FGO is 0.83 nm which corresponds to 2θ=10.6°. It can be concluded from the results of XPS and XRD that both the GO and FGO are prepared successfully.

GO has a bad dispersion in water or common organic solvents. Many researchers have tried to improve dispersion by grafting organic groups and received good results [13,15]. Here, the FGO has a good dispersion in dimehyl sulphoxide and sulfonic acids of FGO can react with imidazolium groups of QPEEK forming ionic bond. Therefore, FGO has an excellent compatibility with QPEEK. As shown in Figure S2, FGO in the QPEEK-5%FGO membrane is well-distributed. However, the QPEEK-5%GO membrane shows a rough and phase-separated appearance. And the cross-sectional SEM morphologies also prove that the compatibility between FGO and QPEEK is great, as shown in Figure 1(d, e). In the cross-sectional image of QPEEK-5%GO, it can be seen that there are many lamellar projections, which is contributed to the lamellar GO. On the contrary, QPEEK-5%FGO membrane has a flat and uniform morphology.

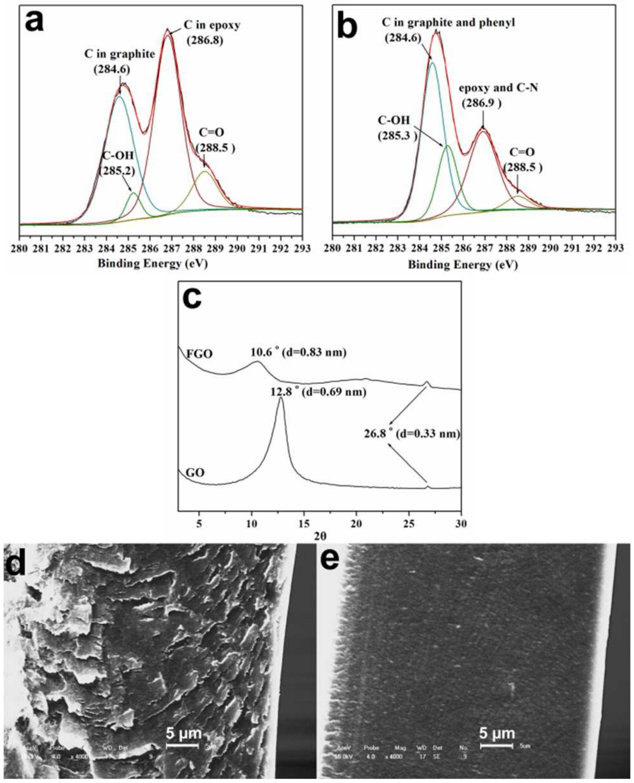

Figure 1. a, b) were the XPS spectra of GO and FGO, respectively; c) was XRD spectra of GO and FGO; d, e) were the cross-section morphologies of QPEEK-5%GO and QPEEK-5%FGO, respectively.

For the PA doped proton exchange membrane, PA acts as both donor and accepter of protons, and thus building the hydrogen bond network for proton conduction. Therefore, the PA doping level is an important factor for proton conductivity. The pristine PA-QPEEK membrane without GO or FGO was excessively swollen and the swelling ratio was not able to be tested. The W_{doping}, $V_{swelling}$ and proton conductivities of PA-QPEEK-*x*%GO and PA-QPEEK-*x*%FGO membranes are shown in Table 1. As shown in Figure 2, the W_{doping} values of PA-QPEEK-*x*%GO and PA-QPEEK-*x*%FGO membranes show a decreasing tendency with the increasing of GO or FGO. This is mainly because the PA absorbing ability of GO and FGO is far lower than that of QPEEK. The PA-QPEEK-*x*%GO membranes have higher W_{doping}, $V_{swelling}$ and proton conductivities than those of PA-QPEEK-*x*%FGO membranes, which should be attributed to the different chemical structure of GO and FGO. There are many oxygen-containing groups on the surfaces of GO. In PA-QPEEK-*x*%GO membranes, the oxygen-containing groups are beneficial to form hydrogen bonds with PA and act as sites for proton conduction. Therefore, besides PA-QPEEK-10%GO, the proton conductivities of PA-QPEEK-*x*%GO membranes increase with the addition amount of GO, although the W_{doping} shows a slightly decreasing. The highest proton conductivity is 74.9 mS cm^{-1} at 200 °C for PA-QPEEK-7%GO. For the FGO, on one side, part of epoxy groups react with p-aminobenzene sulfonic acids, which results in steric hindrance for PA to approach other oxygen-containing groups. On the other side, the sulfonic acids on the FGO react with imidazolium groups, thus forming a cross-linking network structure. These two factors lead PA-QPEEK-*x*%FGO to have lower W_{doping} and proton conductivity than PA-QPEEK-*x*%GO and show decreasing proton conductivity with the introduction of FGO. However, the proton conductivities of PA-QPEEK-*x*%FGO membranes are still higher than that of SGO/PBI/PA membrane, 0.052 S cm^{-1} [12]. Meanwhile, the proton conductivities of PA-QPEEK-*x*%FGO were comparable to those of acid-doped phenylindane-PBI membrane prepared by Benicewicz *et al* [16]. Therefore, both PA-QPEEK-*x*%GO and PA-QPEEK-*x*%FGO have relatively high proton conductivity.

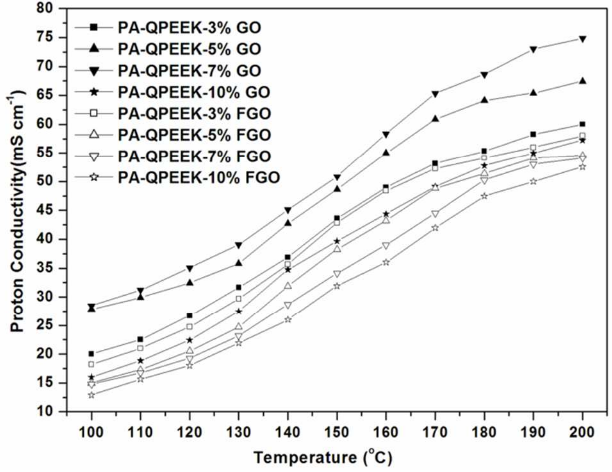

Figure 2. The proton conductivities of PA-QPEEK-*x*%GO and PA-QPEEK-*x*%FGO membranes.

Table 1 The W_{doping}, V_{swelling}, oxidative stability and proton conductivities of PA-QPEEK-*x*%GO and PA-QPEEK-*x*%FGO membranes.

Sample	W_{doping} (wt%)	V_{swelling} (%)	Oxidative stability (h mm^{-1})	Proton conductivity (mS cm^{-1})	
				140 °C	200 °C
PA-QPEEK	—^{a}	—^{a}	—^{a}	—^{a}	—^{a}
PA-QPEEK-3%GO	213	114	85.0	40.9	64.0
PA-QPEEK-5%GO	197	105	109.0	42.7	67.4
PA-QPEEK-7%GO	193	101	113.0	45.1	74.9
PA-QPEEK-10%GO	126	69	124.1	34.7	57.2
PA-QPEEK-3%FGO	189	96	98.6	35.7	58.0
PA-QPEEK-5%FGO	175	81	111.1	31.8	54.5
PA-QPEEK-7%FGO	154	74	126.1	28.7	54.1
PA-QPEEK-10%FGO	109	59	169.2	26.0	52.5

^{a} The membrane had excess swelling and could not be tested.

The ex situ durability test and in situ continuous durability test are used to evaluate the oxidative stability of PEM, in which the ex situ durability test is widely used. In this work, the PA doped membranes were exposed to 3 wt.% H_2O_2, 4 ppm Fe^{2+} Fenton solution in water bath at 80 °C. The breaking time is that the time membrane takes to begin to break into pieces after being shaken. Meanwhile, the thickness of a membrane is considered as a factor influencing membrane breaking. Therefore, the ratio of the breaking time to thickness is used to evaluate the oxidative stability of membrane. The oxidative stability is list in Table 1. It can be seen that the oxidative stability of PA-QPEEK-*x*%GO and PA-QPEEK-*x*%FGO increases with the introduction of GO or FGO, and the PA-QPEEK-*x*%FGO membranes have better oxidative stability than PA-QPEEK-*x*%GO membranes. As we previous reported, the low W_{doping} and the formation of cross-linking structure are beneficial to enhance the oxidative stability [17].

The mechanical properties of all membranes before and after PA doping are listed in Table S1. Figure 3 shows the stress-strain curves of PA doped membranes. It can be seen that the QPEEK-*x*%FGO membranes have higher tensile strength and larger elongation at the break than QPEEK-*x*%GO membranes, which is the result of two factors. First, GO has a worse compatibility with QPEEK than FGO. Second, the cross-linking network in QPEEK-*x*%FGO improves the tensile strength. After being doped with PA, the tensile strength decreases and elongation at the break increases, which is because PA acts as a plastic in the PA doped membrane. The PA-QPEEK-*x*%FGO membranes have relatively higher tensile strength than those of reported work [18]. The highest tensile strength is up to 40 MPa for PA-QPEEK-10%FGO, which was higher than that of PBI-PA membrane [19].

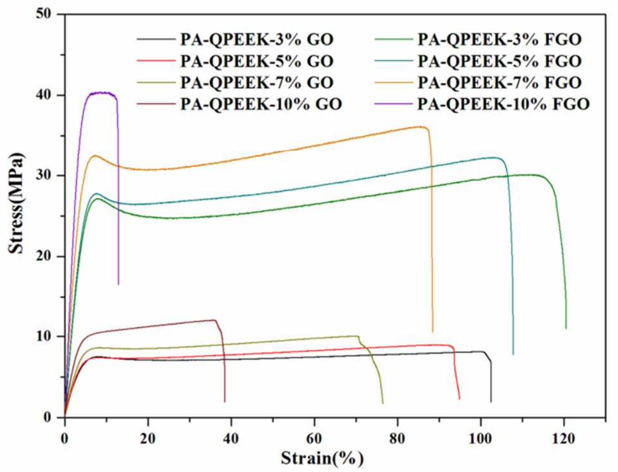

Figure 3. The mechanical properties of PA-QPEEK-*x*%GO and PA-QPEEK-*x*%GO

In summary, the PA-QPEEK-*x*%GO and PA-QPEEK-*x*%FGO used as HTPEMs were prepared successfully. FGO had a better dispersion in organic solvent than GO because of the introduction of organic groups. Meanwhile, the sulfonic acids of FGO reacted with imidazolium groups of QPEEK to form a cross-linking network structure. Therefore, FGO had a better compatibility with QPEEK than GO. After being doped with PA, both PA-QPEEK-*x*%GO and PA-QPEEK-*x*%FGO had excellent dimensional stability. Although the PA-QPEEK-*x*%FGO had slightly lower proton conductivity than PA-QPEEK-*x*%GO, the proton conductivity was still higher than those of reported work. Especially, the tensile strength of PA-QPEEK-*x*%FGO was dramatically improved. The oxidative stability of PA-QPEEK-*x*%GO and PA-QPEEK-*x*%FGO increased with the introduction of GO or FGO. It can be concluded that FGO reinforced PA doped proton exchange membrane could efficiently solve the problem of deterioration in mechanical strength at a high doping level.

The authors acknowledge the financial support from the Natural Science Foundation of China (No. 21104022 & 21374034) and Science and Technology Development Plan of Jilin Province (Grant No. 20130522138JH).

Notes and references

** Corresponding authors*
Alan G. MacDiarmid Institute, College of Chemistry, Jilin University, Changchun 130012, P. R. China. Fax: +86-431-85168870; Tel: +86-431-85168870; E-mail : zhaochengji@jlu.edu.cn; huina@jlu.edu.cn.

[1] J. M. Andújar, F. Segura, *Renew. Sust. Energ. Rew.*, 2009, **13**, 2309-2322

[2] D. Yuan, Z. Liu, S. W. Tay, X. Fan, X. Zhang and C. He, *Chem. Commun.*, 2013, **49**, 9639-9641

[3] (a) S. Bose, T. Kuila, T. X. H. Nguyen, N. H. Kim, K. Lau, J. H. Lee, *Prog. Polym. Sci.*, 2011, **36**, 813-843. (b) J. Zeng, B. He, K. Lamb, R. D. Marco, P. K. Shen and S. P. Jiang, *Chem. Commun.*, 2013, **49**, 4655-4657

[4] Q. Li, J. O. Jensen, R. F. Savinell, N. J. Bjerrum, *Prog. Polym. Sc.*, 2009, **34**, 449-477

[5] (a) M. Li, K. Scott, X. Wu, *J. Power Sources*, 2009, **194**, 811-814. (b) J. Wang, J. Zheng, Z. Zhao and S. Zhang, *J. Mater. Chem.*, 2012, **22**, 22706-22712. (c) J. Yang, Q. Li, J. O. Jensen, C. Pan, L. N. Cleemann, N. J. Bjerrum, R. He, *J. Power Sources*, 2012, **205**, 114-121

[6] (a) C. I. Morfopoulou, A. K. Andreopoulou, M. K. Daletou, S. G. Neophytides and J. K. Kallitsis, *J. Mater. Chem. A*, 2013, **1**, 1613-1622. (b) M. K. Daletou, M.Geormezi, E. K. Pefkianakis, C.Morfopoulou, J. K. Kallitsis, *Fuel cells*, 2010, **10**, 35-44

[7] M. R. Karim, *et al.*, *J. Am. Chem. Soc.*, 2013, **135**, 8097-8100

[8] H. Tateishi, *et al.*, *J. Electrochem. Soc.*, 2013, **160**, F1175-F1178

[9] Ravikumar and K. Scott, *Chem. Commun.*, 2012, **48**, 5584-5586

[10] C.W. Lin, Y.S. Lu, *J. Power Sources*, 2013, **237**, 187-194

[11] Y. He, C. Tong, L. Geng, L. Liu, C. Lü, *J. Membr. Sci.*, 2014, **458**, 36-46

[12] C. Xu, Y. Cao, R. Kumar, X. Wu, X. Wang and K. Scott, *J. Mater. Chem.*, 2011, **21**, 11359-11364

[13] H. Yang, F. Li, C. Shan, D. Han, Q. Zhang, L. Niu and A. Ivaskab, *J. Mater. Chem.*, 2009, **19**, 4632-4638

[14] (a) A. B. Bourlinos, D. Gournis, D. Petridis, T. Szabó, A. Szeri, and I. Dèkàny, *Langmuir*, 2003, **19**, 6050-6055. (b) M. H. Alonso, A. A. Abdala, M. J. McAllister, I, A. Aksay and R. K. Prudhomme, *Langmuir*, 2007, **23**, 10644-10649

[15] S. Stankovich, R. D. Piner, S. T. Nguyen, R. S. Ruoff, *Carbon*, 2006, **44**, 3342-3347

[16] X. Li, X. Chen, B. C. Benicewicz, *J. Power Sources*, 2013, **243**, 796-804

[17] (a) N. Zhang, C. Zhao, W. Ma, S. Wang, B. Wang, G. Zhang, X. Li and H. Na, *Polym. Chem.*, 2014, **5**, 4939-4947. (b) N. Zhang et al., *J. Mater. Chem. A*, 2014, **2**, 13996-14003

[18] (a) J. Kerres, F. Schonberger, A. Chromik, T. Haring, Q. Li, J.O. Jensen, C. Pan, P. Noye, N. J. Bjerrum, *Fuel cells*, 2008, **08**, 175-187. (b) T. H. Kim, T. W. Lim, J. C. Lee, *J. Power Sources*, 2007, **172**, 172-179

[19] K. A. Perry, K. L. More, E. A. Payzant, R. A. Meisner, B. G. Sumpter, B. C. Benicewicz, *J. Polym. Sci., Part B: Polym. Phys.*, 2014, **52**, 26-35